Novel Organic and Inorganic Materials for High Efficiency Electrochemical Energy Storage and Conversion

A Thesis Submitted towards Partial Fulfilment of

BS-MS Dual Degree Program

By

Ajay Kumar

(Registration No. 20111011)

Under the Guidance of

Prof. Satishchandra B. Ogale

Department of Physics and Chair of centre for Energy Science

IISER Pune, India

To

Department of Chemistry

Indian Institute of Science Education and Research (IISER) Pune

CERTIFICATE

This is to certify that this dissertation entitled **"Novel Organic and Inorganic Materials For High Efficiency Electrochemical Energy Storage and Conversion"** towards the partial fulfilment of the BS-MS dual degree programme at the Indian Institute of Science Education and Research, Pune represents the research carried out by **"Ajay Kumar** at IISER Pune" under the supervision of **"Prof. Satishchandra B. Ogale**,Department of Physics and Chair of Centre for Energy Science, IISER Pune," during the academic year **2015-2016**.

Ajay Kumar

Ajay Kumar

Prof. Satishchandra B. Ogale

(Thesis Supervisor)

Date: 23rd April 2016

Place: Pune

DECLARATION

I hereby declare that the matter embodied in the report entitled "**Novel Organic and Inorganic Materials For High Efficiency Electrochemical Energy Storage and conversion**" are the results of the investigations carried out by me at the Department of Physics, IISER Pune, under the supervision of **Prof.Satishchandra B. Ogale** and the same has not been submitted elsewhere for any other degree.

Ajay Kumar

Date: 23rd April 2016

Ajay Kumar

Place: Pune

Reg. No. 20111011

Acknowledgement

I would like to express my heartfelt gratitude and special appreciation to my supervisor **Prof. Satishchandra B. Ogale** for providing me an opportunity to work on my Master's thesis. His highly enthusiastic and positive nature, patience, scientific advice, cooperation, immense knowledge is the key for successful completion of my thesis work in available time frame. By giving excellent environment, freedom which every researcher earnestly desires has not only helped me during the time of master thesis but also developed my thinking ability to become an independent thinker. I would also like to express my deep gratitude to my TAC member **Dr. Sujit K. Ghosh** who has supported me during the course of my master thesis by periodic discussions and motivation which has helped me a lot to complete the task.

I would also like to express my deep gratitude and special thanks to **Mr. Malik Wahid, Dr. Abhik Banerjee and Dr. Dhanya Puthussery** for their kind support and guidance during the course of my work.

I would like to convey my great thanks to **Dr. Shyambo Chatterjee** who has taken care of the synthesis part of polyimides which is reported in the section of synthesis of the polyimides.

I would also like to convey my thanks to all my lab mates Dr. Pradeep, Aniruddha, Rounak, Umesh, Golu, Anil, Dr. Satish, Dr. Monika, Vishal, Vikash, Roma, Kingshuk, Rajesh, Mukta, Dr. Supriya, Dr. Neelima, Poonam, Swati, Srashti, Harshita, Kaustubh, Akash, Ishita, Divya, Dr. Surendra, Dr. Padmini, for their constant support, encouragement and fruitful discussions.

I would also like to acknowledge my IISER friends and teachers who has made possible this important journey of life.

Last but not the least I want thank all my family members without their sacrifice, constant support and encouragement this might not be possible.

Ajay Kumar

Dedicated to my beloved Family and Teachers

CONTENTS

1. Abstract 9
2. Introduction 9
2.1 Energy storage 10
2.2 Lithium Ion Battery 12
2.3 Hydrogen Evolution 15
3. Electrochemical Measurements 17
3.1 Cyclic Voltammetry (CV) 17
3.2 Glavnostatic Charge Discharge 18
3.3 Linear Sweep Voltammetry 20
3.4 Electrochemical Impedance Spectroscopy 21
4. Materials and Methods 23
4.1 Polyimides based Organic Molecules as High Performance Anode Materials for Li ion Battery 23
4.1.1 Synthesis of PTCDA based Polyimide 1 (PI-I) 23
4.1.2 Synthesis of PTCDA based Polyimide II (PI-II) 23
4.1.3 Electrode Preparation for Li ion Battery 26
4.1.4 Coin Cell Fabrication for Testing 26
4.1.5 Results and Discussion 27
4.1.6 Importance of carbonyl group 31
4.1.7 Conclusion 33
4.2 Aligned Nickel Cobalt Phosphide Nano needle arrays uniformly grown on carbon fiber paper: An efficient catalyst for electrochemical Hydrogen evolution 34
4.2.1 Synthesis of Nickel Cobalt Phosphide 34
4.2.2 Results and discussions 35
4.2.3 Electrochemical Performance 38
4.2.4 Electrochemical Measurements 40
4.2.5 Conclusion 40
5. References 41

List of figures

1. Schematic of Mechanistic differences in charge storage of a typical battery and Supercapacitor……11
2. Ragone plot (specific energy vs. specific power) for various energy storage devices…… 11
3. Schematic of li ion battery during charging and discharging……12
4. a) Biologic instrument (b) Autolab Potentiostats (c) Battery Tester……..17
5. Cyclic Voltammogram plot……..18
6. Typical charge discharge plot of battery……19
7. LSV Plots of Different types of MoS_2 and Pt……20
8. Nyquist plot for a Li ion battery anode……...21
9. FTIR spectra of Monomers shows two broad IR peaks at 1774 and 1720 cm^{-1}.24
10. FTIR spectra of Polyimide I (PI-I) and Polyimide II (PI-II)……..25
11. Coin cell fabricated from polyimide material…….. 26
12. Cyclic Voltammetry study if PI-I…… 27
13. Charge Discharge graph of PI-I (1A/g)…… 28
14. Rate performance at different current densities..... 29
15. Impedance measurement…… 30
16. Stepwise lithium insertion free energy (ΔG) for compounds with substituted and unsubstituted carbonyls…… 32
17. SEM images of best performing NCP-400 at different resolution……... 35
18. Compares the surface morphology of NCP samples prepared by at three synthesis temperatures of 300^0C, 400^0C, and 500^0C…… 36
19. Shows the EDAX analysis carried out on three NCP samples prepared at 300^0C, 400^0C, 500^0C……37
20. XRD of NCP-300, NCP-400 and NCP-500 samples…… 37
21. (a) LSV Plots of NCP- 300, NCP-400, NCP- 500 (b) Tafel Plots of NCP- 300, NCP-400, NCP- 500 (c) EIS Nyquist plot NCP- 300, NCP-400, NCP- 500 (d) Cyclic stability of NCP- 300, NCP-400, NCP- 500……39

List of Tables

1. FTIR stretching frequency assignment of Polyimide I (PI-I) and Polyimide II (PI-II)...25

Schemes

1. Synthetic Scheme of Polyimide I (PI-I) and Polyimide II (PI-II)…….. 24

2. Proposed Lithiation process during discharging…….31

Abbreviations

CV	Cyclic voltammetry
PI-I	Polyimide I
PI-II	Polyimide II
EIS	Electrochemical Impedance Spectroscopy
SEM	Scanning Electron Microscopy
XRD	X-ray Diffraction
NCP	Nickel Cobalt Phosphide
MoP	Molybdenum Phosphide
WP	Tungsten Phosphide
MoC2.	Molybdenum Carbide
EC	Ethylene Carbonate
DMC	Dimethylene Carbonate
PC	Propylene Carbonate
Pt	Platinum
SCE	Standard Calomel Electrode
LSV	Linear Sweep Voltammetry

1. Abstract

The thesis is devised to address the two very important energy related aspects of energy storage and hydrogen generation as per the current scientific trend. In the first part of thesis work a new organic Li ion electrode material in the form PTCDA (perylene 3, 4, 9, 10-tetracarboxylic dianhydride) based Polyimide is proposed as highly stable anode material for Li ion energy storage. Higher Li-ion storage compared to other Polyimides is shown to be driven by the presence of carbonyl groups. We got maximum capacity of 800 mAh/g for Anthraquinone based polyimide (PI-I) for the applied current density of 100 mA/g, the high capacity is due to the reaction of carbonyl group with lithium and also with the pi bonds present in the polymer. We also got very good cyclic stability of about 100% of its reversible capacity retention after 100 cycles and more than 85% capacity retention after 500 cycles for the applied current density of 1A/g and 3A/g, respectively.

In the 2nd part of this thesis synthesis of aligned Nickel Cobalt Phosphide (NCP) nano needles on carbon fiber paper for the first time is being demonstrated as an efficient catalyst for HER. The direct hydrothermal growth of the NCP catalyst on carbon fiber paper is shown to compare well with present state of art HER catalysts. The impressive HER parameters including low over potential of 73mV for achieving the HER current density of 10mA/cm^2 and smaller Tafel slope of 55mV/dec are attributed to direct growth of NCP nanowires on the conducting carbon substrate.

2. Introduction

The major concern of the modern society is the climate change due to increase in consumption of non-renewable fossil fuels. The fundamental challenge of 21st century is to secure clean energy supplies and to decrease the dependency on fossil fuels such as coal, oil and natural gas. Major population of this world depends upon these non-renewable fossil fuels. As a consequence limited reserves of fossil fuels are depleting at alarming rate. The use of these fossil fuels have negative impact on the environment as well. Because burning of fossil fuels produces a large amount of carbon dioxide, sulfur

dioxide, nitrogen dioxide, carbon monoxide and much other hazardous gas so there is need to shift to green and clean energy alternatives [1, 2]. At present the two major aspects which are stressed upon as plausible solutions to energy problems is use of energy from cleaner and renewable sources like solar, wind, geo thermal, tidal and hydel energy & use of clean and energy dense fuels like hydrogen. Thus the intense research is underway towards the synthesis of better energy storage materials and synthesis of better catalysts for hydrogen evolution by water breakdown.

2.1 Energy storage

The inherent nature of intermittency and poor power efficiency (energy delivery being too slow or too fast) associated with the use of the renewable sources of type discussed, makes the energy from these source unavailable for any direct use as such. The storage of energy delivered at natural pace and then the delivery at required pace can be effected by energy storage devices like batteries and super capacitors. Thus these energy storage devices have come to forefront and have become the devices of prime importance for last two decades. This has initiated an intense research interest in energy storage materials itself and people are still battling for the best possible one. Two main energy storage devices which have struck the market presently are super capacitors and batteries. These devices can be distinguished on the basis of mechanism of charge storage. The super capacitors employ the principal of potential driven surface storage of electrolyte ions and electrochemical surface redox reactions.

The battery employs the principal of bulk storage based on electrochemical reversible redox reactions encompassing bulk material. Figure 1 displays a mechanistic differences in charge storage of a typical super capacitor and battery. Because of different mechanisms of charge storage and different extent of material employed for charge storage these devices differ in some of the fundamental electrochemical indicators like energy density, power density, cyclic stability, operating voltage etc. There is a well-known plot called Ragone plot (Energy density vs. Power density plot) which describes

the different electrochemical devices on the basis of energy density and power density as shown in figure 2.

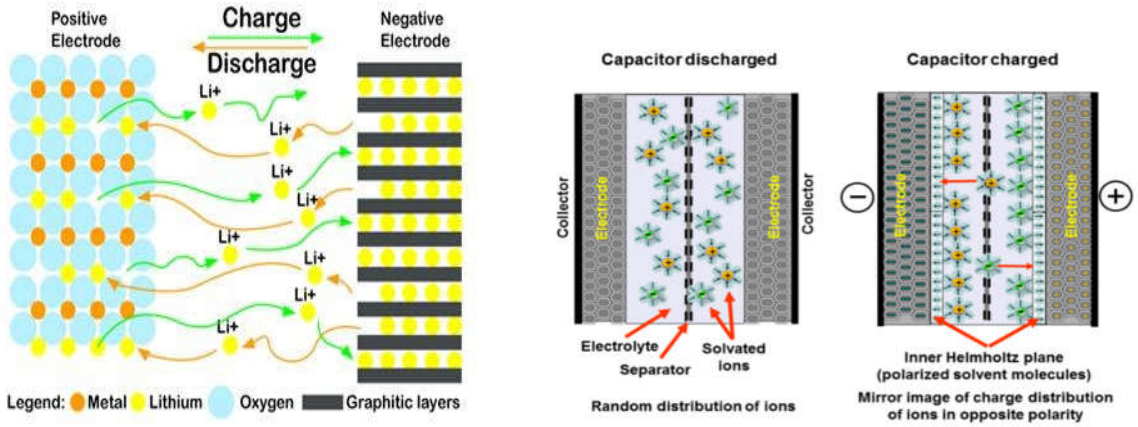

Figure 1. Schematic of Mechanistic differences in charge storage of a typical battery and super capacitor. (Adopted from http://www.cei.washington.edu/education/science-of-solar/battery-technology/ , http://www.wikiwand.com/en/Double-layer_capacitance)

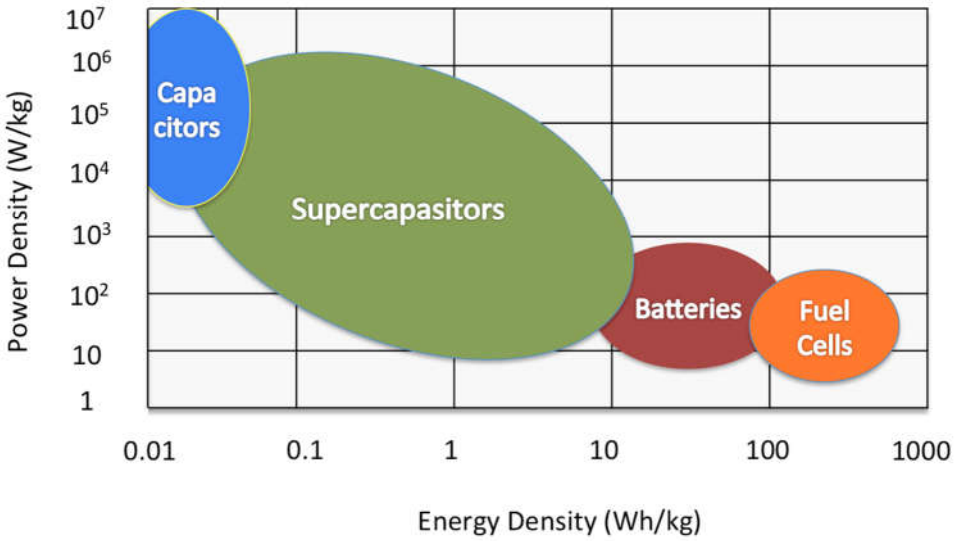

Figure 2. Ragone plot (specific energy vs. specific power) for various energy storage devices. (Adopted from http://large.stanford.edu/courses/2012/ph240/aslani1/)

Being a high energy and average power device the Li-ion battery are currently the dominant energy storage device at market level and it has invited an equally important research status as well. Supercapacitor are only next to Li-ion battery. Li having the highest oxidation potential of all electropositive elements has overtaken all the secondary batteries involving the elements other than a Li. Elaborate explanation of how Li ion is given below.

2.2 Lithium Ion Battery

Rechargeable Lithium ion battery is one of the promising energy storage system for the sustainable use of electrical energy derived from renewable sources. It has a wide range of application from portable electronic devices such as cellular phones, laptops etc. to electric vehicles as well as grid storage, because it offers high energy density among the all existing rechargeable battery technologies [3, 4].

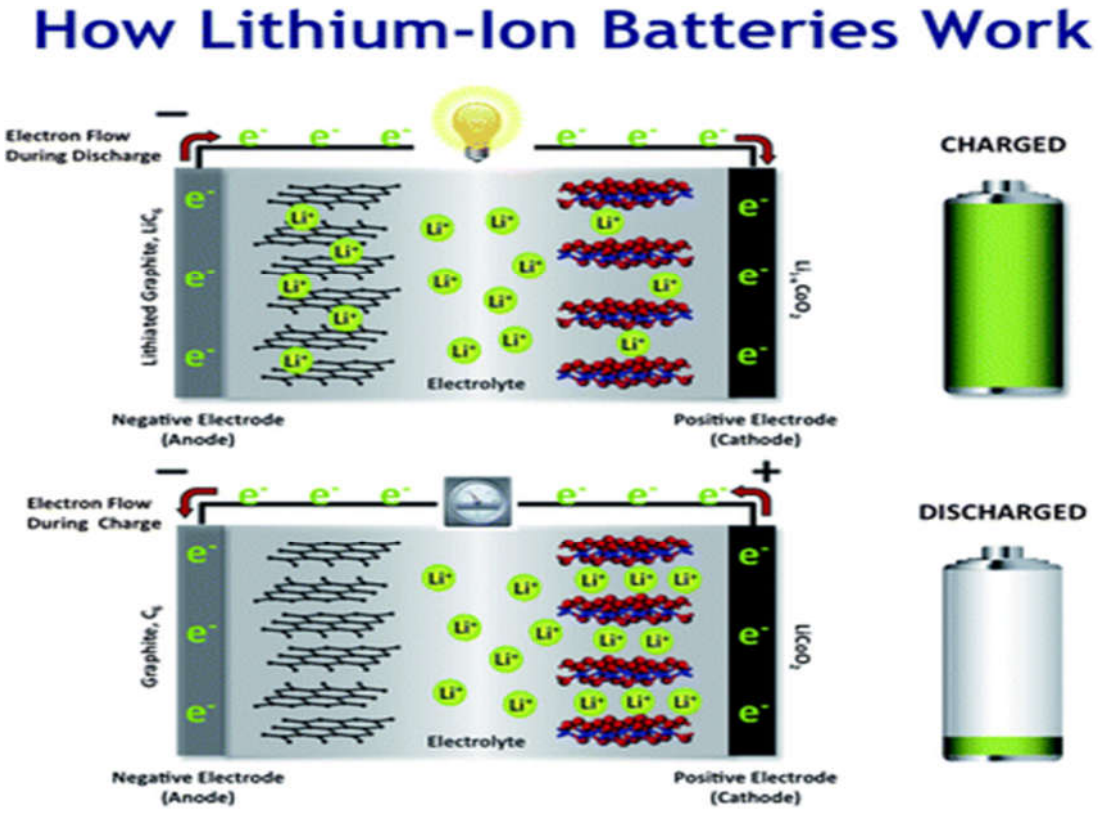

Figure 3. Schematic of Li ion battery during charging and discharging (Reprinted with permission from Ref. 7)

The major components of Li ion batteries are cathode and anode which is separated by an electrolyte usually $LiPF_6$, $LiClO_4$ dissolved in organic carbonates like EC, DMC, PC etc. [5]. The working mechanism of a Li ion battery is shown in figure 3 and explained further with representative example of LiCoO2/ Graphite Li ion battery which happens to be the most famous of all Li-ion commercial batteries [6]. The mechanism involved in Li ion battery are called insertion mechanism. So during electrochemical reaction Li^+ ion are inserted and deinserted while charging and discharging respectively. The cathode materials used in current Li ion battery technology is $LiCoO_2$ from which Li^+ ions are inserted between the layers of graphite (commonly used as anode materials) and forms LiC_6 during charging which then goes back to the cathode materials during discharging [7].

The electrochemical reaction involved during charging and discharging are as follows:

a) At cathode during charging and discharging :

$$LiCoO_2 \underset{\text{Discharging}}{\overset{\text{Charging}}{\rightleftharpoons}} Li_{1-x}CoO_2 + xLi^+ + xe$$

b) At anode during charging and discharging:

$$6C + xLi^+ + xe^- \underset{\text{Discharging}}{\overset{\text{Charging}}{\rightleftharpoons}} LixC_6$$

c) Net reaction after one charge discharge cycle:

$$LiCoO_2 + 6C \underset{\text{Discharging}}{\overset{\text{Charging}}{\rightleftharpoons}} Li_{1-x}CoO_2 + LixC6$$

On the cathode side electrode materials used in conventional Li ion batteries have been Li ion based transition metal oxides like LiNiO2 (Lithium Nickelate), LiMn2O4 (Lithium Manganate) etc.[8,9]. Among all of these $LiCoO_2$ is the best candidate for cathode materials because of its high capacity, reversibility and charge discharge efficiency. The huge research in this field is under way towards the morphology optimization of the already explored cathode materials and toward the exploration of new cathode materials which can have better performance than the existing ones. Other cathode material that has shown promise is $LiFePO_4$, which is shown to have better higher temperature stability than $LiCoO_2$, $LiMn_2O_4$ and others.

The anode side has been the more researched part as the more materials like alloying type such as Silicon, Germanium, Tin etc. which makes alloy with lithium during electrochemical reaction and conversion type materials such as Co_3O_4, Fe_2O_3, Fe_3O_4, CoO, NiO in which oxidation state of the material changes during insertion of Li^+ ions which have showed higher capacity performance than graphite [10, 11]. The graphitic theoretical capacity of 372 $mAhg^{-1}$ is surpassed by the alloying and conversion materials [12]. But there are certain disadvantages of this type of materials such as agglomeration happens in case of alloying type materials as a result, reduction of usage of whole materials with time takes place and cyclic stability is one of the major issue in case of conversion type materials.

Although promising and some of them having already been employed in commercial devices these materials happen to be inorganic and require heavy extraction and processing which renders them costly. Many of these materials are obtained from limited mineral resource. The synthesis of these materials involve high temperature energy intensive ceramic process and generates significant amount of carbon emissions and other hazardous gases [3]. The use of organic alternatives can really be a turnaround in battery technology. Organic molecules based electrode materials are the potential candidate because these are easy to synthesize with low cost as well as eco efficient process [13]. Also these synthetic route provides the flexibility of molecular structure as well as tuning the functional groups. Moreover they are greener and sustainable because many can be prepared from biomass and natural products [3]. The very first use of organic

molecules for electrode materials in batteries was shown by William et al. in 1969 [14]. Several organic molecules such as poly (aniline), Poly (pyrrole), conducting polymers has already been used for secondary Li ion battery [14]. But these all materials has limits in their practical applications due to their thermal instability, cyclic properties, electrode dissolution, poor specific capacities, low crystallinity etc. [14]. The cathode material based on organic small molecule such as NTCDA (naphthalene-tetracarboxylic dianhydride), PMDA (pyromellitic dianhydride), PTCDA (perylene 3,4,9,10-tetracarboxylic dianhydride) has already been explored for Li ion battery due to their high operating potential (1.5 - 4 vs. Li). But this materials also face the same limits such as bad thermal stability, low specific capacities, poor charge discharge stability due to dissolution of small molecules in electrolyte etc. [15]. To get rid of this problem i.e. dissolution in electrolyte thus achieving high capacity one should introduce functional group such as carboxyl group, sulfonic acids or building the polymer with inactive framework which contains redox active units such as aromatic carbonyl [15].

In line with above study we report Polyimide based electrode materials as anode for high performance Li ion battery. These are high performance material due to their mechanical stability, excellent thermo-oxidative properties, electrical property and solvent resistance. These polyimides were synthesized by polycondensation method by incorporating the imide group (CO-N-CO) in the backbone or side chain.

2.3 Hydrogen Evolution

Also considered important for the clean energy is Hydrogen as fuel. It is considered to be one of the solutions along with the energy storage to tackle the global energy problems. Thus electrochemical reduction of water for Hydrogen generation is considered to be integral to several energy technologies which seek for greener and cleaner energy. The energy density of compressed hydrogen is 142MJ/kg and thus is considered as a high density fuel. Apart from some technical handling issues hydrogen holds the promise for sole energy source for the clean and green energy future. Thus photochemical, photo electrochemical, and electrochemical splitting of water into hydrogen and oxygen has been a main focus of research since last few decades. Electrochemical hydrogen

generation is considered the simplest and most promising owing to easy electrode material design. Even though universal catalysts like Pt and other noble metals best catalyze the reduction of water to molecular hydrogen but high cost and least availability of these noble transition metals has led the way open for low cost alternatives from the transition metal series. Various transition metal oxides, sulphides, phosphides, are being reported as efficient catalysts for electrochemical hydrogen evolution reactions. MoS_2, WS_2 are recently gaining importance and are showing the over potentials closer to Pt only. Another stir in the field recently has been the reports of nanostructures of Ni, Co, Fe, Mo, W phosphides for very efficient electrochemical performance. Nickel phosphide nano sheets have shown the over potential of 120mV for the 10mA/cm^2 current with Tafel slope of 79.1mV/dec [16]. Nickel phosphide nanoflkaes have shown over potential of 55mV for 10mA/cm^2 with a Tafel slope of 30mV/dec [17]. Cobalt phosphide with different morphologies and composites like Co_2P/NCNT needs over potential of 406mV for 10mA/cm^2 with Tafel slope of 62mV/dec while CoP /CNT needs only 195mV for 10mV/cm^2 with slope 68mV/dec [18]. We, in this work have tried to club both the transition metals together as a single Phosphide for better HER performance. We in our work on HER are reporting a binary NiCo phosphide nano needles grown on carbon fiber paper as an efficient catalyst. Till now there was no report of any sort on this binary oxide in HER but recently Paik et. al has reported quasi hallow nano cubes which requires over potential of 150mV for 10mA/cm^2 current and over potential of 66.6mV/dec. Our results with the same material with one dimensional needle morphology and direct growth on conducting carbon substrate have delivered a better performance with the requirement of mere 73mV over potential for 10mA/cm^2 and smaller slope of 52mV/dec. The improved performance has been attributed to direct growth of catalyst on the conducting surface which reduces the resistance considerably. The temperature study has been undertaken and it has been observed that NiCo phosphide synthesized at 400^{0}C showing best performance among the all temperature variations studied. Thus Nickel cobalt phosphide nano needles on carbon fiber paper substrate proves to be comparable to and in majority of cases better than most of the present state of art hydrogen evolution catalysts.

3. Electrochemical Measurements

To study the electrochemical performance of the material different electrochemical studies such as CV (Cyclic voltammetry), Glavnostatic charge discharge and electrochemical impedance spectroscopy were performed at room temperature for the prepared battery samples. The characterization was done using Biologic Potentiostats and battery tester as shown in figure 4.

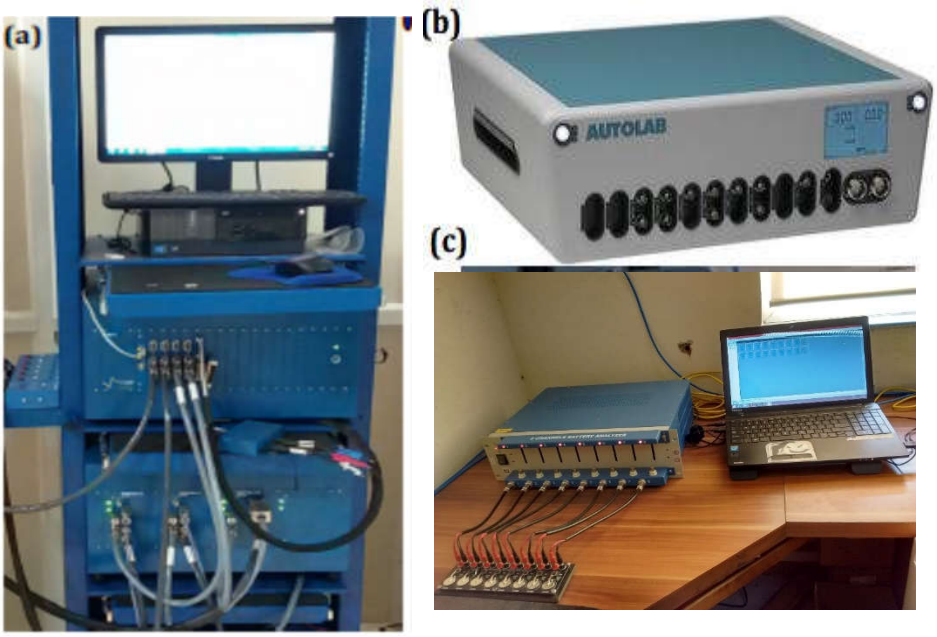

Figure 4. (a) Biologic instrument (b) Autolab Potentiostats (c) Battery Tester (Ref. Lab instrument)

3.1 Cyclic Voltammetry (CV)

Cyclic voltammetry is the most common and very useful technique used in electrochemistry to get the various information of the redox reactions such as oxidation and reduction potential, reaction kinetics and reversibility of the redox reaction in various electrochemical systems such as batteries, Supercapacitor, water splitting etc. [19]. In CV, at a fixed rate, voltage is varied between working electrode and reference electrode from V1 to V2 in time interval t1 to t2. The constant rate at which the voltage varies is also

called scan rate measured in voltage/ second (v/s). When the voltage of working electrode reaches to the maximum set potential (V2) then ramp is reversed back into the initial set potential (V1) from time t2 to t3. The current is measured between counter electrode and working electrode with change in potential. The CV (current vs. voltage) Plot of a single electron transfer for a fixed scan rate are shown in figure 5. When the voltage reaches to the maximum set potential (V2) then it is reversed into the initial set potential (V1). The oxidation and reduction takes place during reverse scan w.r.t each other. The voltage at which maximum peak current appears refers to the standard reduction potential of the material.

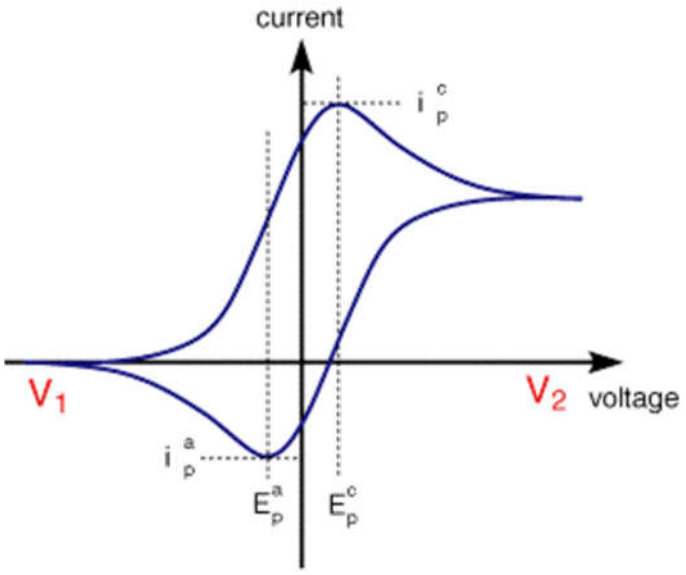

Figure 5. Cyclic Voltammogram plot, where i_p^c and i_p^a refers to cathodic and anodic peak current respectively and E_p^c and E_p^a denotes the corresponding potential (Adopted from http://www.ceb.cam.ac.uk/research/groups/rg-eme/teaching-notes/linear-sweep-and-cyclic-voltametry-the-principles)

3.2 Glavnostatic Charge Discharge

This technique is extensively used for electrochemical systems such as batteries and Supercapacitor to find their charge discharge capacity and cyclic stability of the materials. In this technique variation in potential with time is measured by applying constant current

between working electrode and counter electrode. Figure 6 shows the voltage vs. capacity plot of charge discharge for battery.

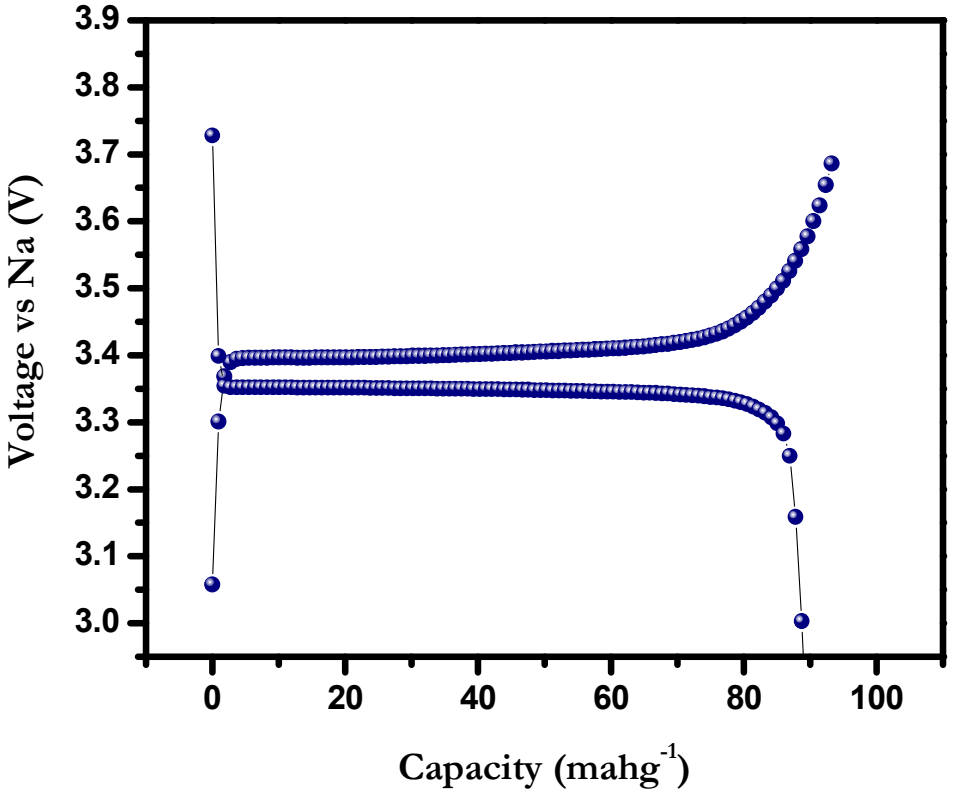

Figure 6 Typical charge discharge plot of battery

The potential window for which the charge discharge is carried out depends upon the electrode materials, electrolyte used etc. from the above graph we get the charge discharge capacity of the material experimentally. Theoretically we get the charge discharge capacity of the Li ion battery electrode materials with the help of the following equations:

$$\text{Capacity (in mAhg}^{-1}) = \frac{n*f}{Molecular\ wt.*3.6}$$

Where, n= no of Li ion stored per molecule

F= Faraday's constant (96500C)

3.3 Linear Sweep Voltammetry

Linear sweep voltammeter is a potential sweep technique in which current response of a sweeping potential is recorded as a graph. It is a modern and advanced version of classical paleography technique. Electro active species in the vicinity of the electrode respond to changing potential. When the potential applied at interface reaches the Standard redox potential of the species there would be current response at that potential. The magnitude of current is a quantitative measure of amount of electro active species present and half wave potential is qualitative measure for material as it is concentration independent.

$$E_{1/2} = E^{o}_{O/R} - (0.05916/n) \log (K_O / K_R)$$

LSV has found use in the characterizing materials for ORR (Oxygen Reduction Reaction), OER (Oxygen Evolution Reaction) and HER (Hydrogen Evolution Reaction) purposes. The characteristic of the LSV measurement is current obtained at different potentials. For a good catalyst material current recorded at particular potential for above reactions is higher than a non-catalyst. Another characteristic of the LSV plot is $E_{1/2}$ which is characteristic for a reaction and for the reactions mentioned it determines the onset potential for the reaction catalyst combination. Figure 7 shows the LSV plot for the universal catalyst and MoS_2 for HER.

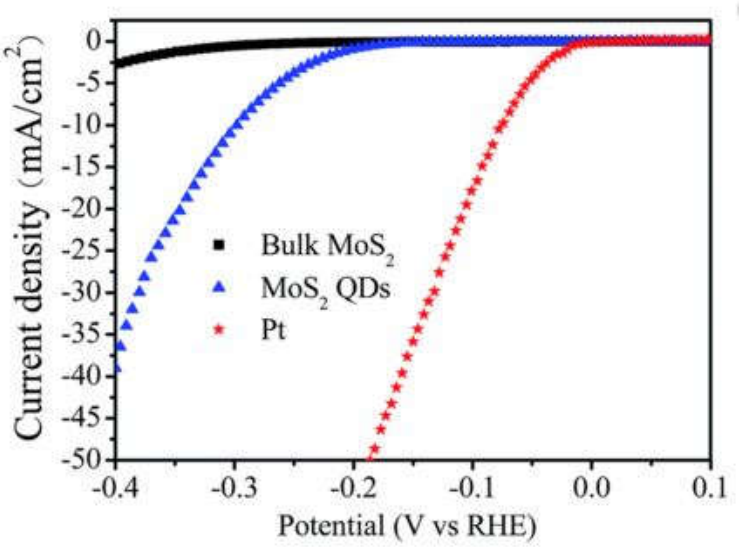

Figure 7. LSV Plots of Different types of MoS_2 and Pt. (Reprinted with permission from ref. 20)

As can be seen the Pt/c delivers a high current densities at lower over potentials than MoS_2 and the onset potential for Pt/C is also lower [20]. Same applies to ORR reactions. Thus LSV is an important tool for electrochemists to explore the material electrochemistry.

3.4 Electrochemical Impedance Spectroscopy

The Impedance spectroscopy has become a powerful tool to characterize the electrochemical systems. The technique comes under the broad domain of ac voltammetry. The word spectroscopy has been associated with it owing to analogy with traditional optical spectroscopic techniques. Here an AC voltage pulses is imposed on a electrochemical system as input and the current response of the system is measured as output. In this technique the impedance is being measured as a function of frequency. The ac voltage pulse being characterized by frequency the impedance comes out to be frequency dependent. The impedance is a generalized ac resistance of a LCR circuit given by equation of Ohms type:

$$Z = \frac{V}{I} = \frac{V^{\circ}e^{i\omega t}}{I}$$

Where Z is impedance and it embodies the complex relation of voltage and current which are out of phase with each other. The following equation relates the impedance of a RC circuit with the resistive and capacitive components

$$Z_{R+C} \text{ in series} = R + \frac{1}{i\omega C}$$

Phase angle (ϕ) between the voltage and current in RC circuit is given by:

$$\tan(\phi) = Z_{im}/Z_{Re} = \frac{1}{\omega RC}$$

Where Z_{im} is imaginary part of resistance and Z_{Re} is real part of resistance.

Frequency dependence of impedance is of immense interest for electrochemists and has been utilized for deriving very important fundamental information regarding electrochemical systems and devises like Lithium ion batteries ,capacitors, Fuel cells, Electro catalytic water splitting etc. The important parameters from EIS which have proven instrumental toward electrochemical understanding include electrochemical series resistance (ESR), Charge transfer resistance, Warburg impedance and others [21]. The two fundamental frequency dependent impedance plots which are of importance to electrochemists are Bode plot, in which log /Z/ and ф are both plotted against log ω and Nyquist plot, which displays Z_{Im} vs. Z_{Re} for different values of ω . Figure 8 displays a Nyquist plot for a Li ion battery anode as a representative example and the EC parameters which can be derived from the plot are listed.

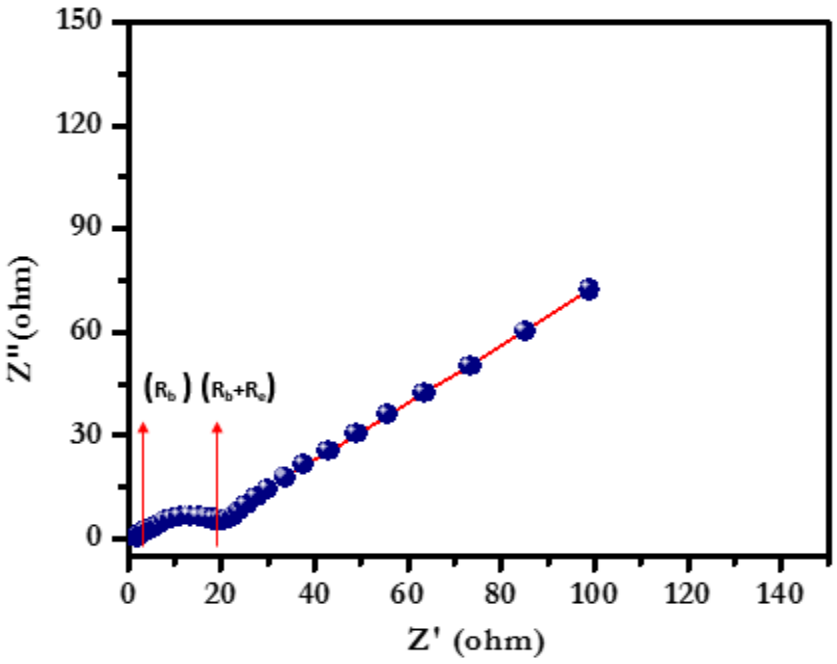

Figure 8. Nyquist plot for a Li ion battery anode

Here, (R_b) refers to the series resistance of the system which includes the resistance of the electrode, current collector and electrolyte. Charge transfer resistance in the Nyquist plot at the interfaces is given by the diameter of each semicircle (R_e).

4. Materials and Methods

4.1 Polyimides based Organic Molecules as High Performance Anode Materials for Li ion Battery

Polyimidization has been done by taking most commonly used 3,4,9,10-perylenetetracarboxylic dianhydride (PTCDA), 2,6-diaminoanthraquinone and 2,6-diaminonapthelene as starting materials. During polyimidization anhydride functionality of PTCDA converts into imide groups and CO are left intact which is very much important for reversible Li+ insertion/deinsertion. Synthesis of Polyimide I (PI-I) and Polyimide II (PI-II) which is described below has been done by Dr. Shyambo Chatterjee, at National Chemical laboratory (NCL), India.

4.1.1 Synthesis of PTCDA based Polyimide 1 (PI-I)

0.50 mmol PTCDA (0.2 g), 0.50 mmol 2, 6 diaminoanthraquinone (0.119 g) and 2 mmol of zinc acetate were allowed to mix in benzimidazole at room temperature under nitrogen atmosphere. After this mixture was kept for stirring at 140^{o}C for 6h, then it was refluxed at (240^{o}C) under nitrogen for 12h. It resulted in viscous solution. After this the resulting viscous solution was left for cooling at room temperature. When it was cooled down to room temperature then it was precipitated in H_2O, filtered and washed repeatedly with DMSO until the DMSO solution became clear. Drying of the sample was done in vacuum at 150ºC for 20h. FTIR measurement was taken for the obtained product, IR (KBr) Vmax: 1699.5, 1670.9, 1667.8, 1588.8, 1506.7, 1348.6, 1247.7, 1165.61, 844.1, 742.7 cm^{-1}.

4.1.2 Synthesis of PTCDA based Polyimide II (PI-II)

0.50 mmol PTCDA (0.2 g), 0.50 mmol 1, 5-diaminonapthelene (0.079 g) and 2 mmol of zinc acetate were allowed to mix in benzimidazole at room temperature under nitrogen atmosphere. After this mixture was kept for stirring at 140^{o}C for 6 h, then it was refluxed

at (240°C) under nitrogen for 12h. It resulted in viscous solution. After this the resulting viscous solution was left for cooling at room temperature and When it was cooled down to room temperature then it was precipitated in H_2O, filtered and washed repeatedly with DMSO until the DMSO solution became clear. Drying of the sample was done in vacuum at 150ºC for 20h. FTIR measurement was taken for the obtained product, IR (KBr) Vmax: 1699.5, 1664, 1595.8, 1506.7, 1411.3, 1344.6, 1247.7, 1022.2, 789.7, 748.7 cm^{-1}.

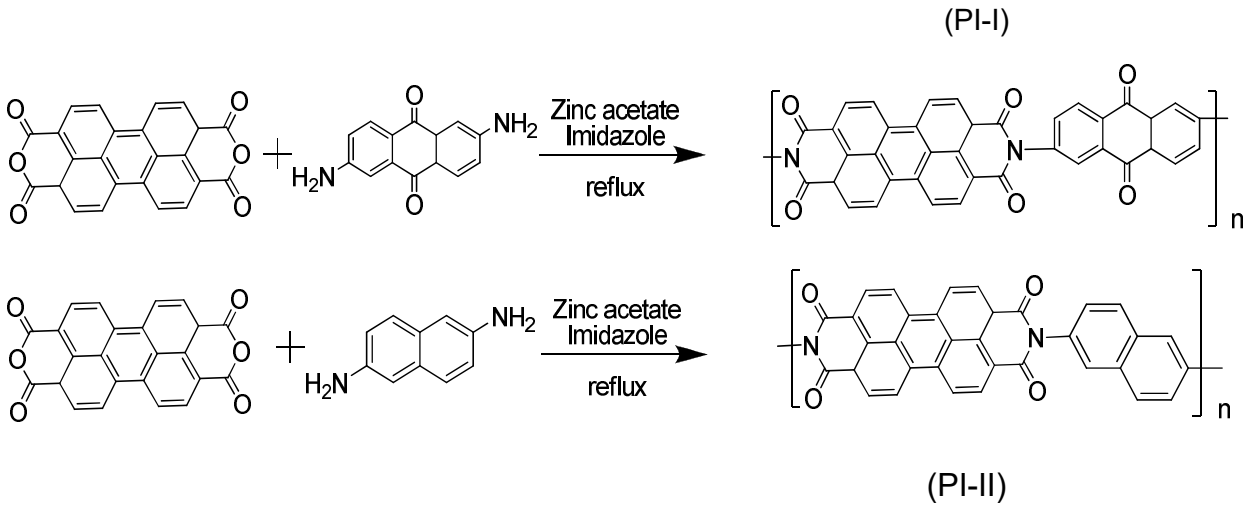

Scheme 1. Synthetic Scheme of Polyimide I (PI-I) and Polyimide II (PI-II)

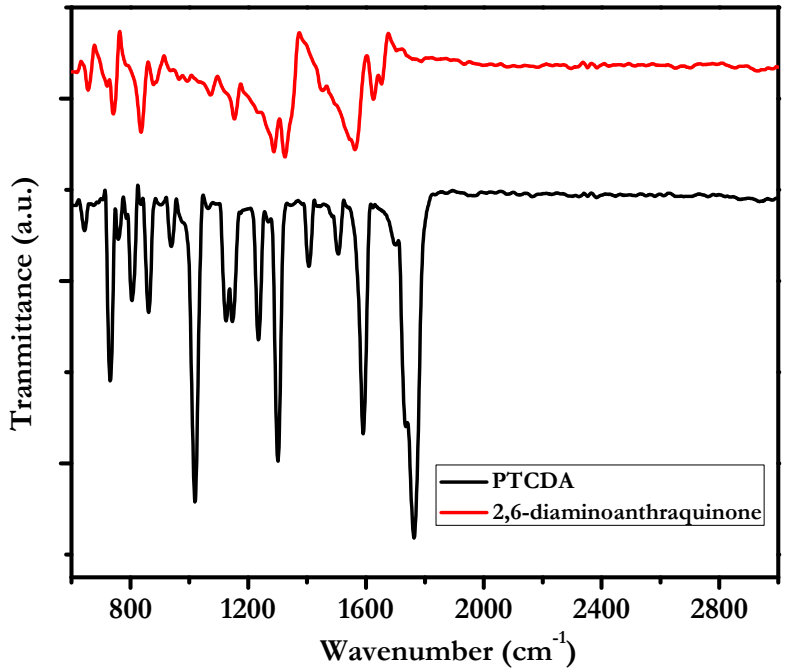

Figure 9. FTIR spectra of Monomers shows two broad IR peaks at 1774 and 1720 cm^{-1}.

We were unable to characterize the PI-I and PI-II by NMR because of very poor solubility. So the imidization was confirmed via FTIR spectroscopy. PTCDA shows two broad IR peaks at 1774 and 1720 cm^{-1} which corresponds to CO symmetric and asymmetric stretching frequency respectively as shown in the figure 9. After the polyimidization absence of 1774 cm^{-1} vibrational IR peaks in PI-I and PI-II as shown in figure 10 directly infers the conversion of anhydride functionality of PTCDA into imide functionality.

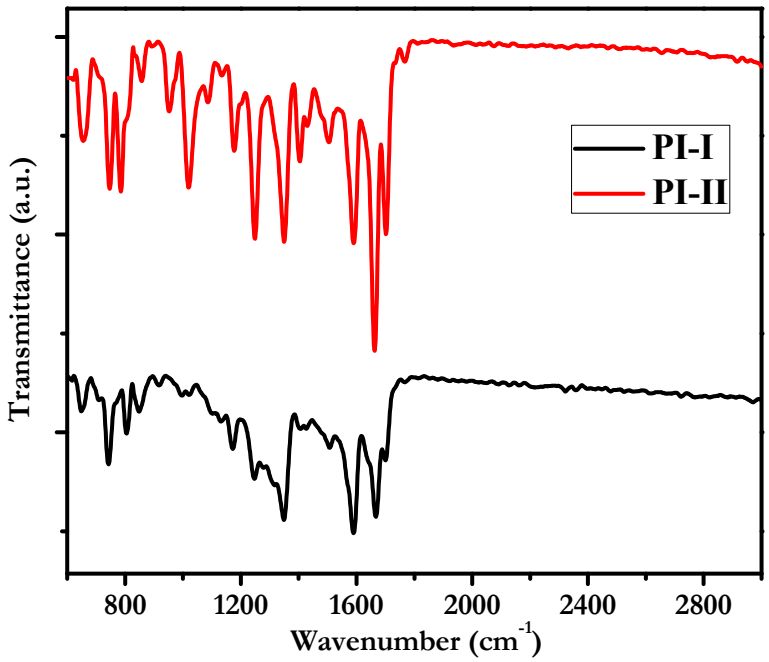

Figure 10. FTIR spectra of Polyimide I (PI-I) and Polyimide II (PI-II)

Group	PI-I	PI-II
Imide C=O, ν_{as}	1699.5	1699.5
Imide C=O, ν_{s}	1667.8	1659.7
Imide C-N, ν	1348.6	1344.6
Imide C=O, δ	742.7	746.8

Table 1. FTIR stretching frequency assignment of Polyimide I (PI-I) and Polyimide II (PI-II).

4.1.3 Electrode Preparation for Li ion Battery

Electrode for different electrochemical measurements was prepared using 70 wt.% of material (PI), 20 wt.% conducting carbon (Super P) and 10 wt.% binder (PVDF, sigma Aldrich) was mixed homogeneously by using NMP as a solvent in agate mortar. The obtained slurry was coated homogeneously on copper foil. After this it is kept for drying at room temperature for 8hrs. After drying at room temperature for 8hrs it was put in oven at 75ºC for 12h. for complete drying.

4.1.4 Coin Cell Fabrication for Testing

The prepared electrode on the copper foil was cut into round shape and size of 2032 type coin cell. This 2032 type coin cell was fabricated inside argon filled glove box (with the level of oxygen less than 0.1 ppm). The various components used in the coin cell are working electrode on copper foil, Li metal (0.75 mm thickness) used as counter electrodes, separator (Porous Polypropylene membrane, Celgard), Stainless steel current collector (Spacer), and 1M $LiPF_6$ in Ethylene Carbonate (EC) / Diethyl carbonate (DEC) Mixture (1/1, w/w, BASF) as electrolyte. The fully fabricated coin cell is shown in figure 11.

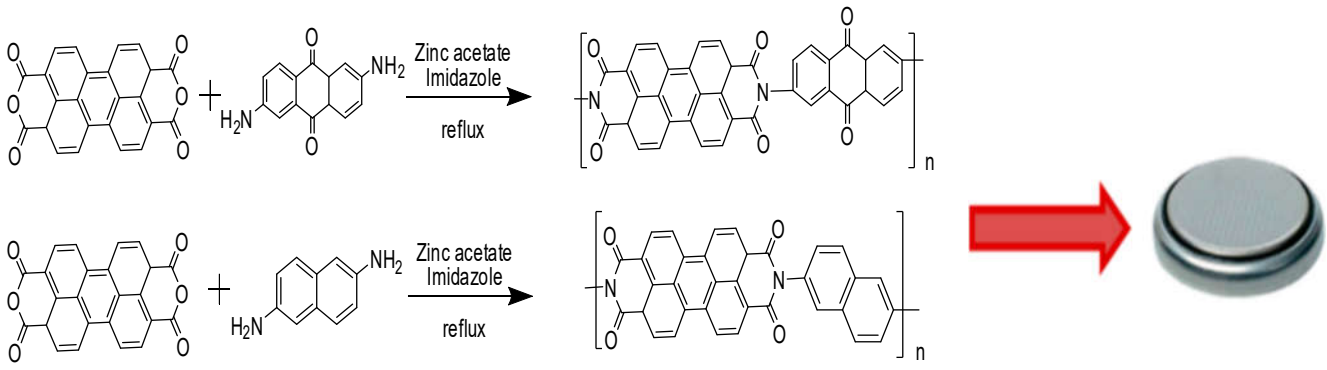

Figure 11. Coin cell fabricated from polyimide materials

4.1.5 Results and Discussion

Polyimidization reaction has been done by mixing the monomers in stoichiometry amount in the high boiling point solvent or mixture of solvent at 180-220°C [22-25]. The imidization was confirmed via FT IR spectroscopy. PTCDA shows two broad IR peaks at 1774 and 1720 cm^{-1} which corresponds to CO symmetric and asymmetric stretching frequency respectively. After the polyimidization absence of 1774 cm^{-1} vibrational IR peaks in PI-I and PI-II directly infers the conversion of anhydride functionality of PTCDA into imide functionality.

To study the performance of Li ion battery for synthesized polyimide different electrochemical studies such as CV (Cyclic voltammetry), charge discharge, impedance spectroscopy were performed at room temperature. All the measurements were studied with the help of 2032 coin cell of synthesized polyimide with Li metal as reference electrode.

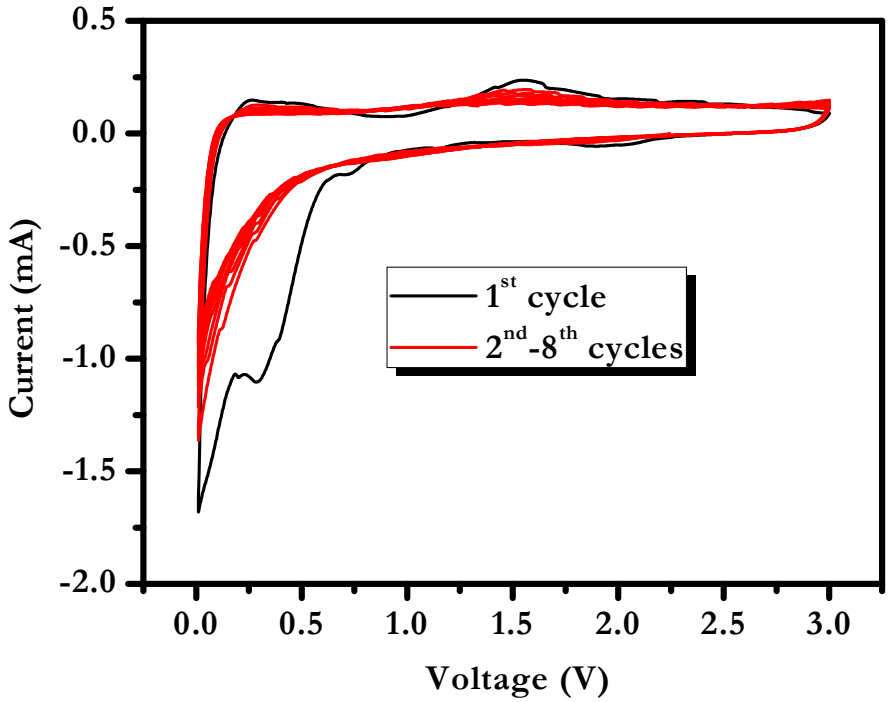

Figure 12. Cyclic Voltammetry study of (PI-I)

Figure 12 shows the CV of synthesized polyimide (PI-I) within the potential window of 0.01-3V with the scan rate of 0.1mV/sec. From the figure we can see the peak at 2V

during the first cathodic scan which corresponds to enolization reaction of lithium with the oxygen of carbonyl group of polyimide, which has already been explored in earlier study. Along with this peaks there are other reduction peaks at the position 0.28, 0.7 and one close to zero which corresponds to the SEI (Solid electrolyte interface) and lithiation of pi bond of carbon. We also observed the peak at around 1.5V during anodic scan which is the result of delithiation process.

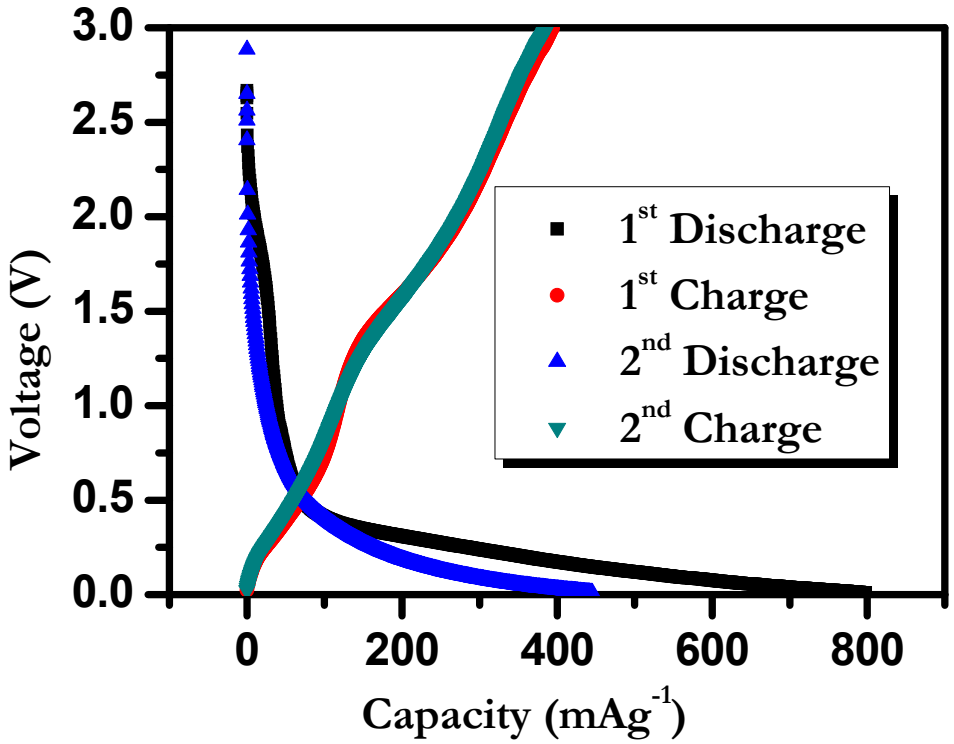

Figure 13. Charge Discharge graph of PI-I (1A/g)

Figure 13 shows the charge discharge graph of synthesized polyimide (PI-I) with applied current density 1A/g upto a voltage of 0.01V vs. lithium. Upto 2V a sharp decrease in potential is seen, after that a small plateau was observed at 2V, which corresponds to enolization reaction of four oxygen of carbonyl with Lithium. The Charge discharge profile follows the CV nature of synthesized polyimide (PI-I). From the graph we can see that the first discharge capacity is 798mAh/g, while the charge capacity is decreases up to 394mAh/g with a columbic efficiency of only 49%. This is because of the formation of SEI (Solid electrolyte Interface) due to the decomposition of organic electrolyte. This

phenomena is common for the almost all anodic first discharge profile. The second discharge capacity is 434mAh/g while the charge capacity is 386mAh/g with a columbic efficiency of about 88%. After about 100 cycles we see almost 100% capacity retention with reversible capacity of about 429mAh/g with stable cyclic performance. This high capacity is because of high material participation, low solubility of material in electrolyte etc. The low solubility of material is confirmed by taking FTIR of liquid (here electrolyte) which was mixed with polyimide. We see the peak which corresponds to functional group of electrolyte while we didn't see any Vibrational peak which corresponds to any of functional group of polyimide.

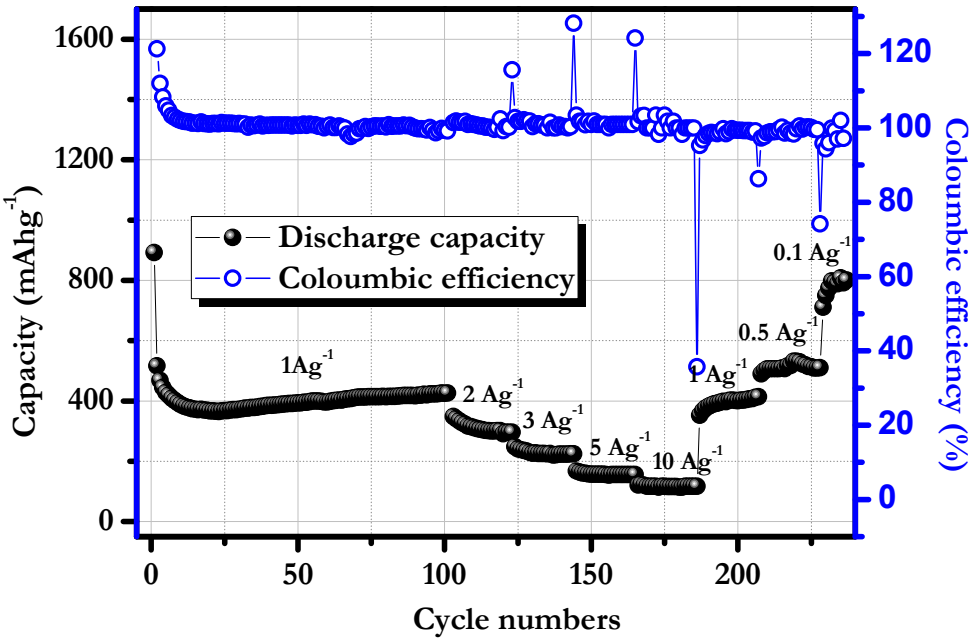

Figure 14. Rate performance at different current densities.

Figure 14 shows the rate performance of Polyimide (PI-I) cell at different current densities. The same cell was used for rate performance which was cycled up to 101 charge discharge cycles. The maximum capacity of the polymer at the current density 1A/g, 2A/g, 3A/g, 5A/g and 10mAh/g are 425 mAh/g, 348 mAh/g, 247 mAh/g, 225 mAh/g and 121 mAh/g respectively. This shows that the Polyimide (PI-I) exhibits high capacity retention at high current density which is far better than the many reported organic small molecules

After checking the rate performance of the cell at high current density, the cell was again checked at low current density which results in the retention of capacity. The maximum capacity of polyimide at low current density of 0.5 A/g and 0.1A/g are 531 and 807mAh/g respectively, which is higher than the already reported organic compounds and several inorganic anode materials.

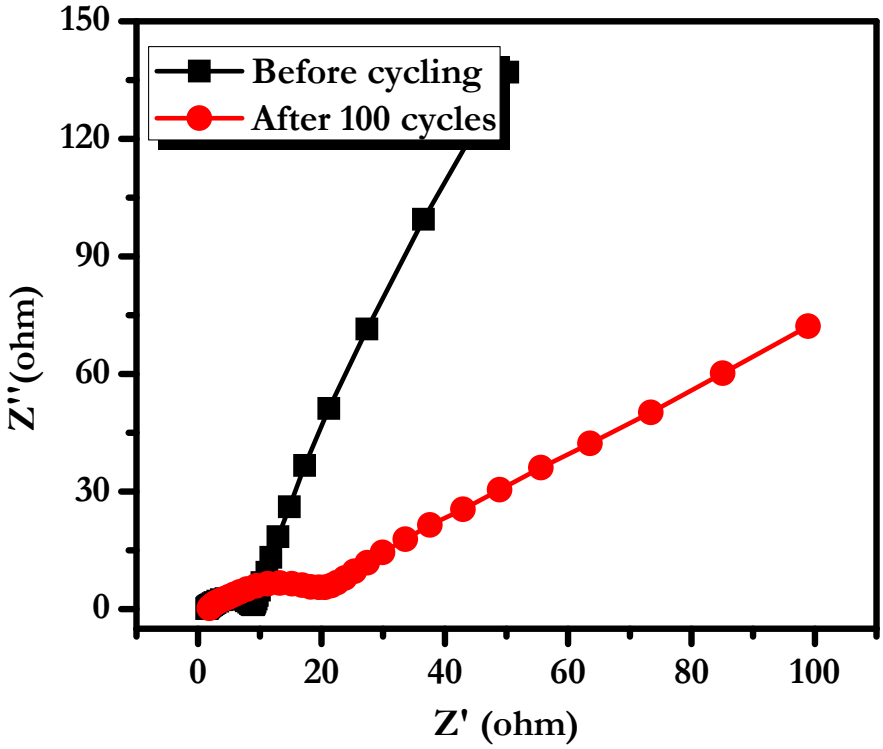

Figure 15. Impedance measurement.

Figure 15. Shows the impedance spectroscopy analysis of Polyimide (PI-I) cell before and after 100 cycles. The initial resistance is called Warburg resistance which is due to diffusion of Li ion in the material. The end point of the semicircles refers to the charge transfer resistance. In the figure we can see that the charge transfer resistance of initial cycle is 9 ohm which increases to 20 ohm after 100 cycles, which is because of the SEI formation due to decomposition of electrolyte. This resistance is in fact less than many of the reported polymer based anode as well as some inorganic base anode material for Li ion battery application. The high capacity of polyimide (PI-I) obtained is not only due to participation of only carbonyl group, because if there would be participation of only

carbonyl group then maximum capacity comes out to be 277mAh/g. Thus result of high capacity and discharge potential window is less than the usual is due to participation of carbonyl as well as alkene bond present in PI-I as shown in scheme 2. If every carbonyl as well as pi bond reacts with lithium during discharging i.e. 42 lithium ion per formula unit then maximum theoretical capacity comes out to be 1756 mAh/g. But the obtained capacity is less than the theoretical. This is possibly due to dead kinetics of some pi bond at room temperature as suggested by Wu et al. where he got less capacity of the polymer than the expected one.

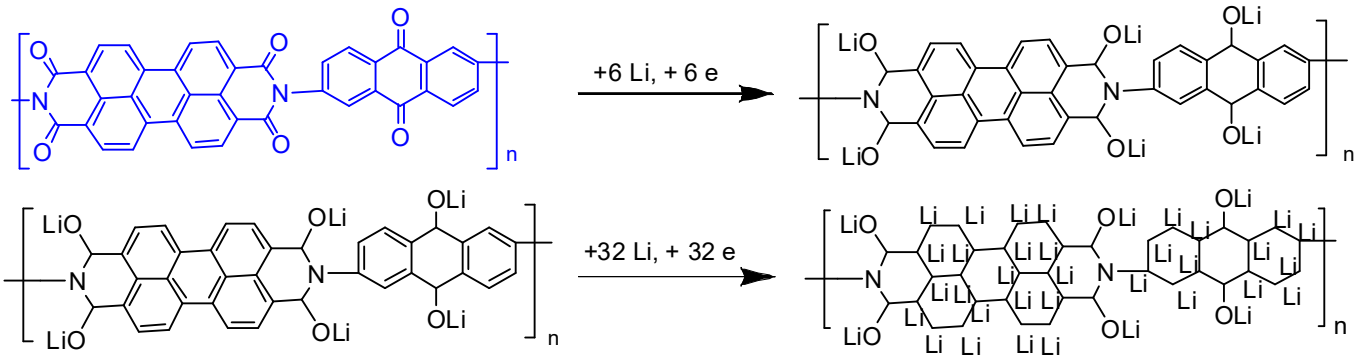

Scheme 2. Proposed Lithiation process during discharging

4.1.6 Importance of carbonyl group

It was first observed by Han et.al. that capacity of polymer with fused rings where all pi bonds undergoes lithiation (Li ion insertion in C6 ring) process is influenced by presence of carbonyl group [26]. This was further explained by him by theoretical approach, which tells that the free energy of the polymer which has carbonyl functional group is less than the one which doesn't has carbonyl group. They have explained it through DFT calculation depicted in figure 16, which shows that stepwise reaction of lithium insertion has lower free energy in case of compound with anhydride groups than compounds such as NTCDA than with unsubstituted aromatic ring compound such as Pyrene and Naphthalene [26].

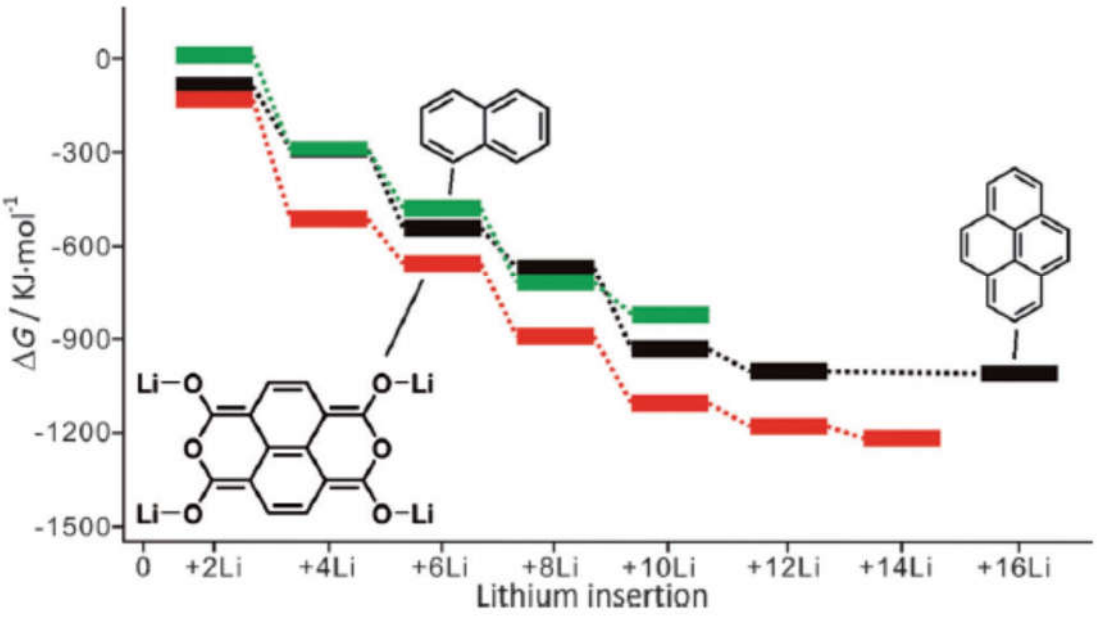

Figure 16. Stepwise lithium insertion free energy (ΔG) for compounds with substituted and unsubstituted carbonyls (Ref. 26. X. Han, G. Qing, J. Sun and T. Sun, *Angew. Chem. Int. Ed*. **2012**, 51, 5147 –5151)

So lower the free energy more the lithiation as a result we get the high capacity. To check the influence of carbonyl group for our materials, we replace 2,6-diaminoanthraquinone with 2,6-diaminonapthelene and polyimidization is done with PTCDA, and this polyimide is named as PI-II. The cell of PI-II was made with same loading as that of PI-I. The PI-II cell has been tested for cyclic performance with applied current density of 1A/g , the reversible capacity obtained is 126mAh/g which is one third of the reversible capacity of carbonyl functionalized polyimide (PI-I). So we can say that PI-I has the high reversible capacity than PI-II, this is due to presence of carbonyl functional group in PI-I, which enhances the capacity.

4.1.7 Conclusion

In conclusion, we have successfully synthesized two different aromatic polyimide which has been done using a high temperature solution imidization process using PTCDA, 1, 4-diaminoanthraquione and 1, 4-diaminonaphthalene, respectively for the application of anode materials for Li ion battery. The polyimide which has formed through imidization of PTCDA and 1, 4-diaminoanthraquione showed the better result as compared to the polyimide formed through imidization of PTCDA and 1, 4-diaminonaphthalene. The better performance of the former is due to presence of carbonyl group which reduces the free energy (ΔG) of lithium insertion reaction [12]. So in this study we have also shown the importance of carbonyl group in enhancing the reversible capacity than the unfunctionalized one. As a result we got maximum capacity of 800 mAh/g for anthraquinone based polyimide (PI-I) for applied current density of 0.5 A/g and 126mAh/g for naphthalene based polyimide (PI-II) for the applied current density of 1A/g. This polyimides shows better performance as compared to various organic small molecules conjugated ladder polymer (81 mAh g^{-1} for around 2.4 A g^{-1} and almost no capacity for 4, 6 and 12 A g^{-1}) as well as several reported inorganic metal oxides such as CuO (210 mAh g^{-1} at high current rate of 2 A g^{-1}), Fe_2O_3 (206 mAh g^{-1} at current rate of 2 A g^{-1}), sulfide, based nanostructures and alloy based compounds [27,28-32].

4.2 Aligned Nickel Cobalt Phosphide Nano needle arrays uniformly grown on carbon fiber paper: An efficient catalyst for electrochemical Hydrogen Evolution

4.2.1 Synthesis of Nickel Cobalt Phosphide

Carbon fiber paper was sonicated in de-ionized water for half an hour before use. 4 mmol (950.7 mg) of nickel chloride hexahydrate ($NiCl_2.6H_2O$ from Merck) 8 mmol (1903 mg) of cobalt chloride hexahydrate ($CoCl_2.6H_2O$ from Merck) and 15 mmol (900.9 mg) of urea (CH4N2O) was taken in a beaker and mixed it with 80 ml deionized water and kept for stirring for half an hour until it becomes clear pink colored solution. This solution was transferred to a 100 ml Teflon lined autoclave. The carbon fiber paper with the supported with glass slide was dipped at an angle into the Teflon lined stainless steel autoclave. The solution containing autoclave was sealed in kept in electric oven at temperature 125ºC for six hours. After six hours it was allowed to cool down naturally room temperature. A pink colored film was formed on the fiber paper. After this the obtained deposited film was subjected to phosphorisation to obtain NCP (Nickel cobalt phosphide) by annealing them at 300ºC, 400 ºC and 500ºC for 2h by passing sodium hypophosphite and argon gas mixture through a split tube furnace to obtain NCP- 300, NCP- 400 and NCP- 500 samples.

4.2.2 Results and discussions

The SEM images of best performing NCP samples which was annealed at 400 ºC was shown in figure17.

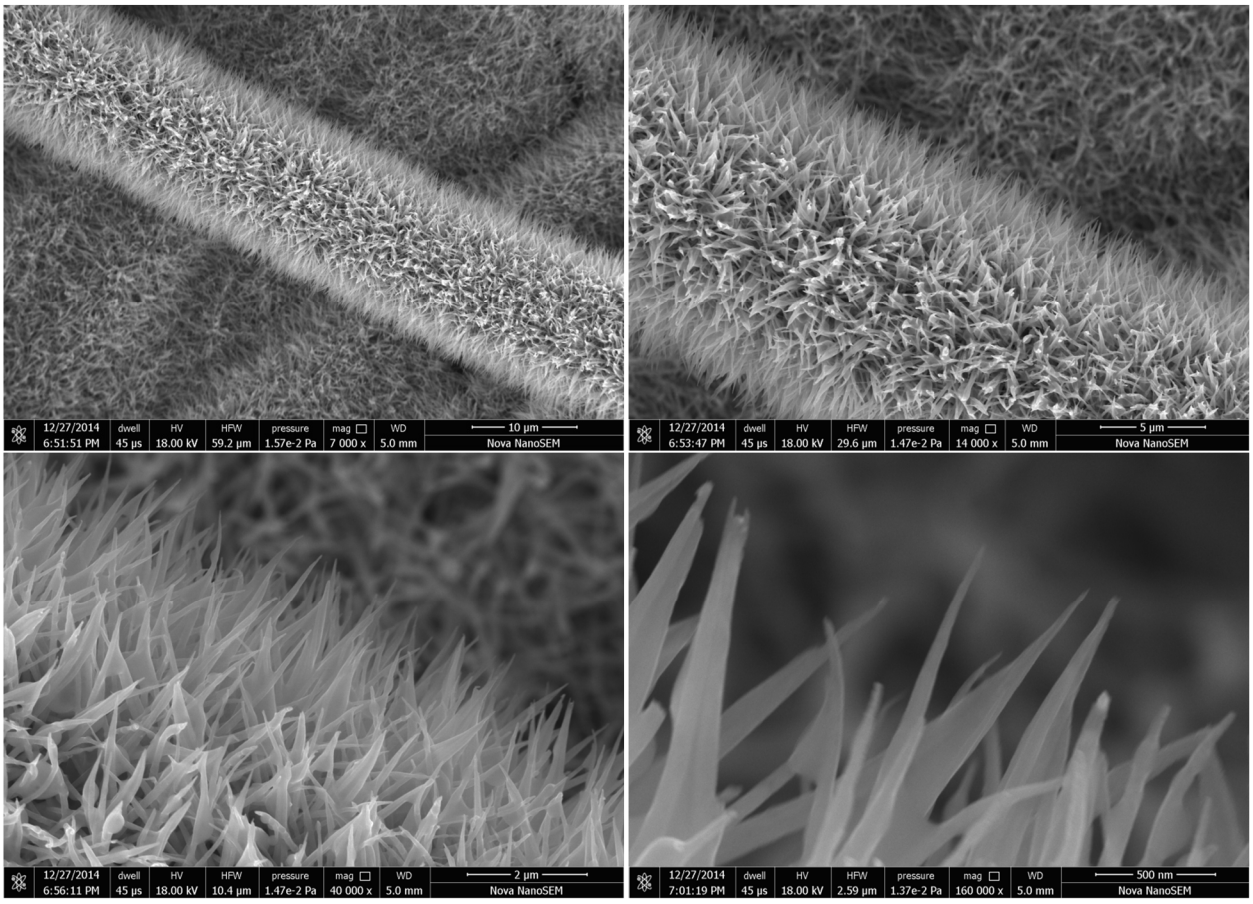

Figure 17. SEM images of best performing NCP-400 at different resolution

Figure 17 shows the needle type of morphology and uniform growth of needles over the fibers of carbon support. The particular morphology with a broad base and tipped end offers the advantage of high surface area and thus possibility of maximum exposed catalytic sites. The availability of maximum catalytic sites in turn enhances TOF (turn over frequency) of catalyst. Figure 18 compares the surface morphology of the three samples prepared at 300^0C, 400^0C, 500^0C. The long needle type morphology of Ni-Co precursor for (phosphorisation reaction) is perfectly retained in the NCP-300 and NCP-400, but phosphorisation at 500^0C leads to collapse of the morphology which in turn leads to

closure of paths towards active HER site and hence in lowered HER performance in NCP-500.

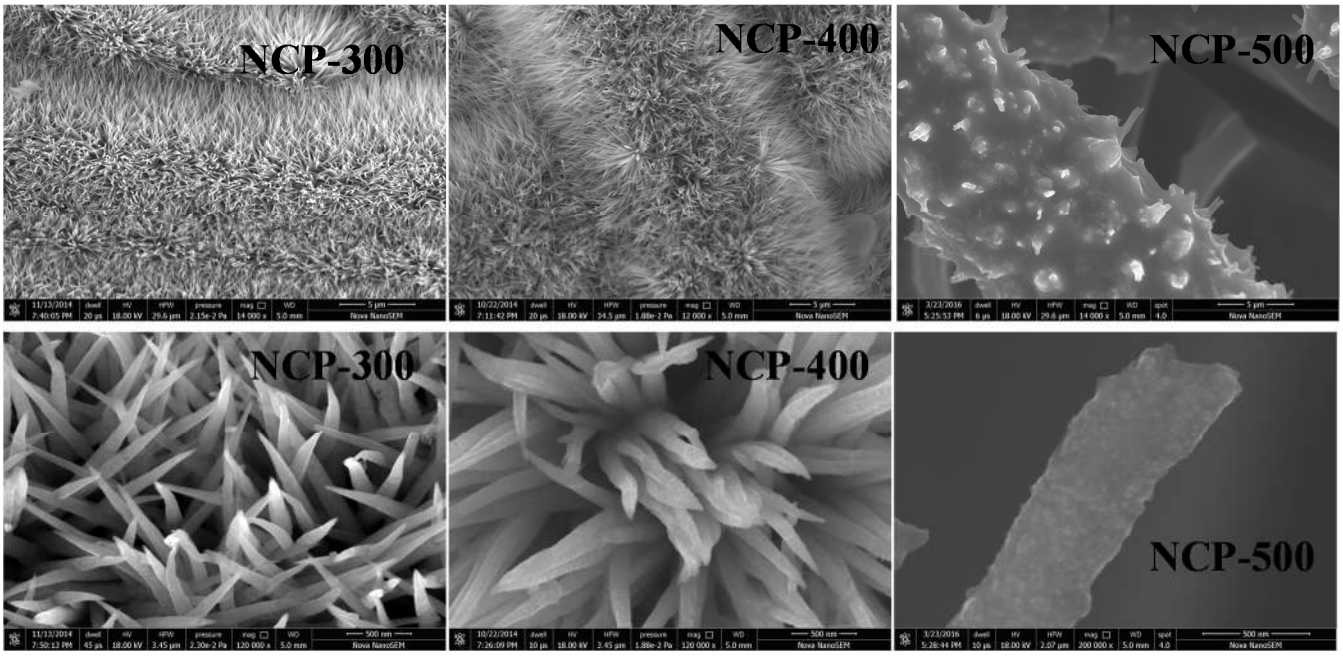

Figure 18. Compares the surface morphology of NCP samples prepared by at three synthesis temperatures of 300^0C, 400^0C, and 500^0C.

Composition analysis by EDAX shown in figure 19 reveals that phosphorisation seems to be temperature dependent. Total metal to phosphorus atomic ratio being 1:1 (approx.) for NCP-300, and being 1:1.5 (approx.) for NCP-400 and NCP-500. The XRD plot (Figure 20) further supports the observation through the presence of precursor peaks below 21^0. The HER performance has been seen sensitive to metal to sulphur ratio and metal to phosphorus ratio in transition metal oxides already [33, 34]. Thus combination of metal to phosphide ratio and surface morphology projects NCP-400 as the best for HER performance among the three synthesized material samples.

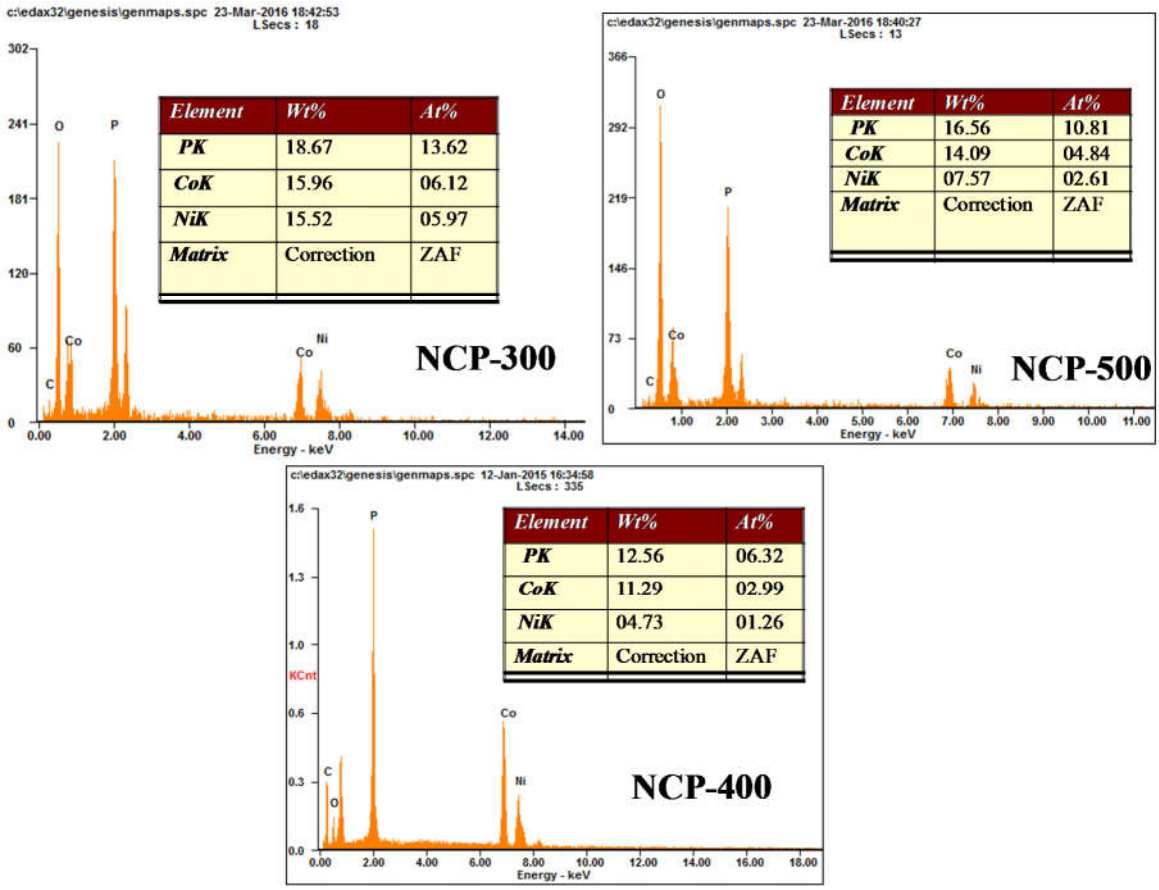

Figure 19. Shows the EDAX analysis carried out on three NCP samples prepared at 300^0C, 400^0C, and 500^0C

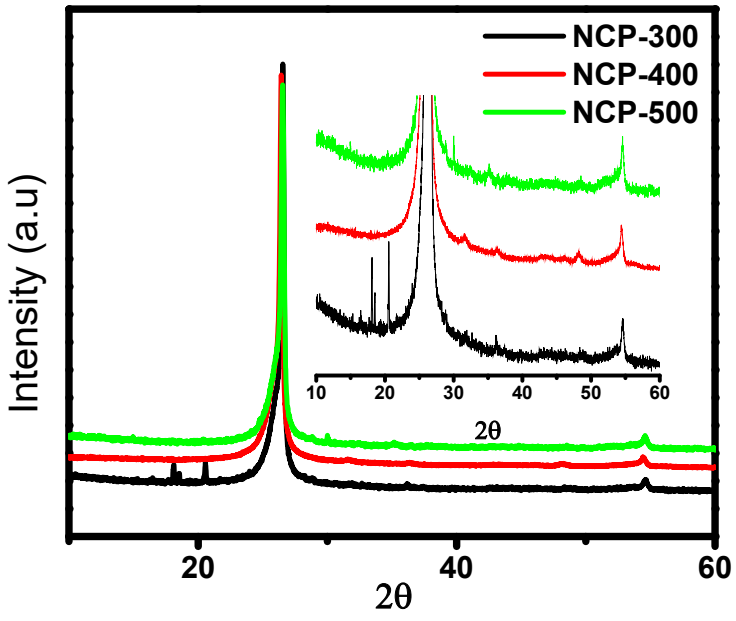

Figure 20. XRD of NCP-300, NCP-400 and NCP-500 samples.

4.2.3 Electrochemical Performance

Electrochemical HER activities of the NCP samples prepared under different synthesis conditions (NCP- 300, NCP- 400, and NCP- 500) is shown in Figure 21. All measurements are carried out in 0.5M H_2SO_4 aqueous solution against Hg/Hg_2Cl_2 reference electrode and Platinum as reference electrode. The presented data is IR corrected and converted to RHE scale for final conversion LSV plots. Figure 21(a) shows the comparative performance of three samples. The $10mA/cm^2$ of cathodic current (hydrogen evolution current) is reached at fairly low over potentials of 96mV, 80mv and 71mV respectively for NCP-300, NCP-500 and NCP-400 respectively. The best performing catalyst happens to be Nickel Cobalt phosphide which is struck by 400^0C phosphorization temperature in our synthesis. Further a comparison at $100mA/cm^2$ for different samples also reveals the best performance shown by NCP-400. The over potentials required for generation of $100mA/cm^2$ are 185mV, 155mV, 126mV respectively for NCP-500, NCP-300, NCP-400 respectively. Comparisons at two current densities for our NCP-catalyst (NCP-400) shows superior performance compared to Ni only counter parts like Nickel phosphide nanoflakes, nickel phosphide nanosheets, and cobalt only counterparts like Cobalt phosphides (CoP and Co_2P) [16-18]. The Over potential values for generation of $10mA/cm^2$ compare well with Commercial Pt/C (20%) for which the value being 59mV**.** [18].

Figure 21(b) shows the Tafel analysis for the three samples it can be seen that low Tafel slopes are observed. NCP-400 displays the Tafel slope of 48mV/dec, compared to 56mV/dec and 266mV/dec for NCP-300 and NCP-500. Lower Tafel slopes imply the Heyrovsky mechanism where proton dissociation is rate determining step. And in the case of NCP-500 the higher slope implies Volmer mechanism (Hydrogen adsorption being the limiting step) which can be attributed to lack of coordinative electron transfer to Hydrogen ion adsorption due to lost proximity between Ni, Co and phosphide.

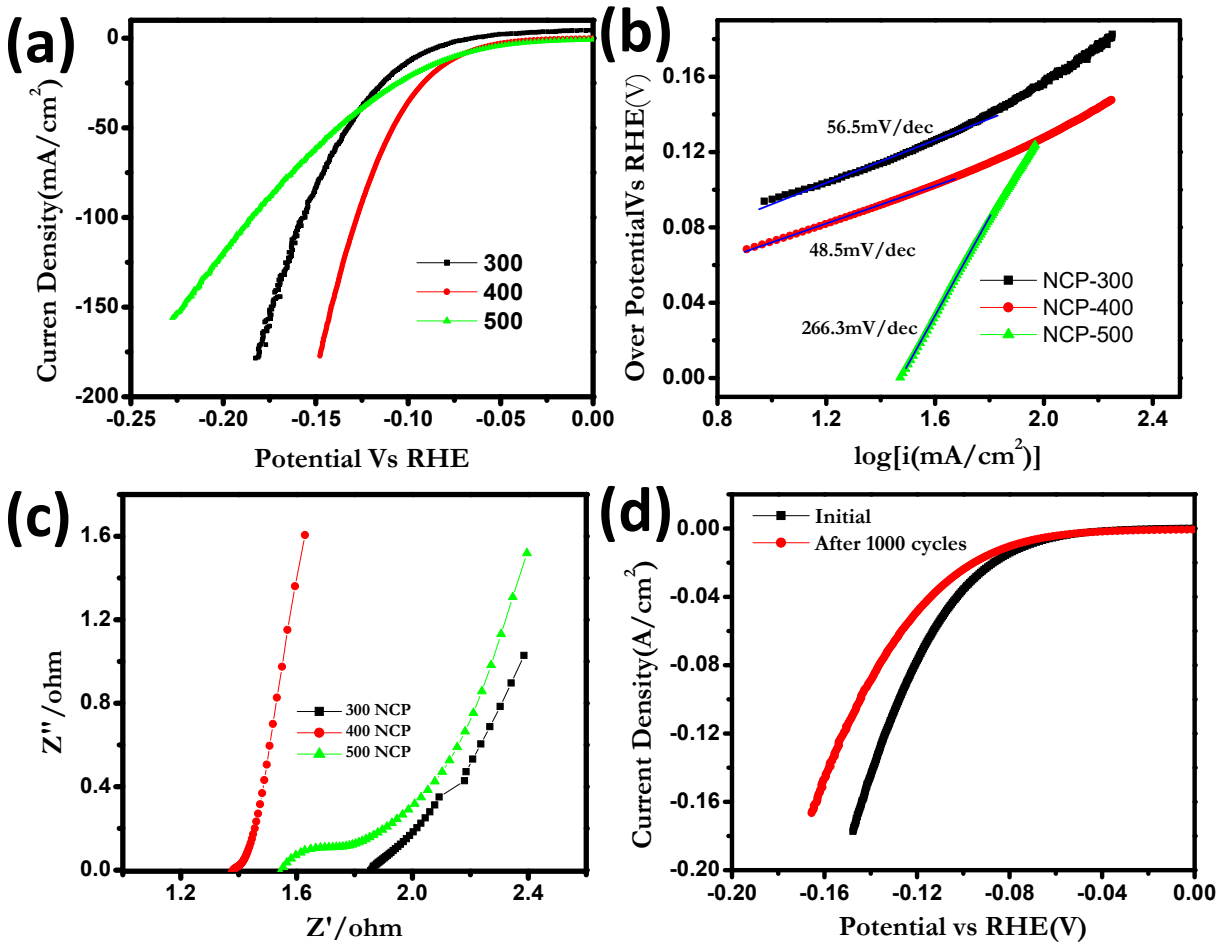

Figure 21. (a) LSV Plots of NCP- 300, NCP-400, NCP- 500 (b) Tafel Plots of NCP-300, NCP-400, NCP- 500 (c) EIS Nyquist plot NCP- 300, NCP-400, NCP- 500 (d) Cyclic stability of NCP- 300, NCP-400, NCP- 500.

Better performance of NCP-400 is further implied by low series resistance and charge transfer resistance of NCP-400 compared to NCP-300 and NCP-500 well brought out by Impedance plot in Figure 21(c) Further Figure 21(d) depicts the excellent stability of NCP-400 catalyst as there is small decrease in catalytic activity after 1000cycles. The over potential required for generation 100mA/cm^2 increases to 144mV from127 mV for fresh catalyst.

4.2.4 Electrochemical Measurements

Electrochemical measurement of LSV and impedance were carried out in three electrode assembly with NCP material grown on Carbon fiber paper as working electrode directly. A 3cm x 1cm platinum was used as counter electrode and Hg/Hg_2Cl_2 (SCE) was used as reference electrode. All measurements were carried out in Autolab potentiostat. The polarization curves obtained were IR corrected by using the resistances from impedance measurements. The conversion of potential axis vs. SCE to RHE was done by employing following equation:

$$E\ (RHE) = E\ (SCE) + 0.059\ p\ H + 0.242\ V.$$

4.2.5 Conclusion

NCP grown on carbon fiber paper performs better than the recently reported NCP quasi Nano hallow boxes and far better than other state of art Ni only and Co only Phosphides reported. Our results are also far superior to some of the recently reported MoP, WP, and MoC2. The superior performance is successfully being explained to be due to special reaction conditions being employed. The particular synthesis method allows better binding with the substrate and one dimensionality which allows high surface area to be exposed and which in turn exposes maximum number of catalytic active sites to electrolyte.

5. References

[1] R. Zeng, L. Zing, Y. Qui, Y. Wang, W. Huang *Electrochimica Acta* **2014**, 146, 447-454.

[2] H. Chen, M. Armand, M. Courty, M. Jiang, C.P. Grey, F. Dolhem, J.M. Tarascon and P.Poizot, *J.Am.Chem.Soc.,* **2009**, 131, 8984-8988.

[3] W. Walker, S. gurgeon, O. Mentre, S. Laruelle and J. M. Tarascon, and F. Waudi, *J.Am.Chem.Soc.*, **2010**, 132, 6517-6532.

[4] L. Wang, H. Zang, C. Mou, Q. Cui, Q. Deng, J. Xiu, X. Dai, J. Li*, Nano Res*.**2015**, 8(2), 523-532.

[5] B. Dunn, H. Kamath and J.-M. Tarascon, *Science*, **2011**, 334, 928-935.

[6] Michael M. Thackeray, Christopher Wolvertonb and Eric D. Isaacsc *Energy Environ. Sci*., **2012**, 5, 7854.

[7] D. Aurbach, *Journal of Power Sources*, **2000**, 89, 206–218.

[8] T. Hutzenlaubz, S. Thiele, R. Zengerle, C. Ziegler, *Electrochem. Solid-State Lett*. **2012**, 15, 33-36.

[9] E. Hosono , T. Kudo , I. Honma , H. Matsuda , H. Zhou, *Nano Lett*., **2009**, 9, 1045–1051.

[10] C.-M. Park, J.-H. Kim, H. Kim and H.-J. Sohn, *Chem. Soc. Rev.*, **2010**, 39, 3115-3141.

[11] P. Poizot, S. Laruelle, S. Grugeon, L. Dupont and J. M. Tarascon, *Nature*, **2000**, 407, 496-499.

[12] P. Poizot, S. Laruelle, S. Grugeon, L. Dupont and J. M. Tarascon, *J. Power Sources*, **2001**, 97–98, 235-239.

[13] M. Chen, F. Armand, G. Demailly, F. Dolhem, P. Pizot and J. M. Tarascon, *ChemSusChem* **2008**, 1, 348 – 355.

[14] H.H. Lee, Y. Park, K.H. Shin, K.T. Lee and S.Y. Hong *Appl. Mater. Interfaces* **2014**, 6, 19118−19126.

[15] B. Haupler, T. Hagemann, C. Friebe, A. Wild, U.S. Schubert, *ACS Appl. Mater. Interfaces* **2015**, 7, 3473−3479.

[16] X. Wang, Y. V. Kolen'ko, X.-Q. Bao , K. Kovnir and L. Liu, *Angew.Chem. Int.Ed.* **2015**, 54, 8188 –8192.

[17] A. Han, S. Jin, H. Chen, H. Ji, Z. Sun and P. Du, *J. Mater. Chem. A,* **2015**, 3, 1941–1946

[18] Yuan Pan, Yan Lin, Yinjuan Chen, Yunqi Liu* and Chenguang Liu, *J. Mater. Chem. A,* 2016, 4, 4745–4754

[19] R. S. Nicholson, *Anal. Chem.*, **1965**, 37, 1351-1355.

[20] X. Ren, L. Pang, Y. Zhang, X. Ren, H. Fan and S. Liu *J. Mater. Chem. A*, **2015**, 3, 10693–10697

[21] M. Toupin, D. Bélanger, I. R. Hill and D. Quinn, *J. Power Sources*, **2005**, 140, 203-210

[22] N. Asano, M. Aoki, S. Suzuki, K. Miyatake, H. Uchida, M. Watanabe, *J. Am. Chem. Soc.*, 2006, 128, 1762 – 1769.

[23] T. Takekoshi, *Polyimides- Fundamentals and Applications*, Ed. M.K. Ghosh, and K.L. Mittal, Marcel Dekker, New York, 1996, Chapter 2.

[24] Bessonov, M.I., Koton, M.M., Kudryavtsev, V.V. and Laius, L.A. *Polyimides: Thermally Stable Polymers, 2nd edition*, Plenum, New York, 1987.

[25] F.W. Harris, *Polyimides*, Ed. D. Wilson, H.D. Stenzenberger, P.M. Hergenrother, Chapman and Hall, New York, 1990, Chapter 1.

[26] X. Han, G. Qing, J. Sun and T. Sun, *Angew. Chem. Int. Ed*. **2012**, 51, 5147 –5151.

[27] J. Wu, X. Rui, C. Wang, W.-B. Pei, R. L. Q. Yan and Q. Zhang*, Adv. Energy Mater*, **2015**, 140, 2189.

[28] X. Han, C. Chang, L. Yuan, T. Sun and J. Sun, *Adv. Mater.*, **2007**, 19, 1616–1621.

[29] A. Banerjee, U. Singh, V. Aravindan, M. Srinivasan and S. Ogale, *Nano Energy*., **2013**, 6, 1158–1163.

[30] A. Banerjee, V. Aravindan, S. Bhatnagar, D. Mhamane, S. Madhavi and S. Ogale,*Nano Energy*, **2013**, 5, 890–896.

[31] Y. Wang, J. Wu, Y. Tang, X. Lu, C. Yang, M. Qin,F. Huang, X. Li, and X. Zhang, *ACS Appl. Mater. Interfaces*, **2012**, 4, 4246−4250.

[32] X. Zhou, J. Bao, Z. Dai and Y.-G. Guo, *J. Phys. Chem. C,* **2013**, 117, 25367−25373.

[33] J. S.-Jirkovský, C. D. Malliakas, P. P. Lopes , N. Danilovic , S. S. Kota , K.-C. Chang B. Genorio, D. Strmcnik , V. R. Stamenkovic , M. G. Kanatzidis and N. M. Markovic, *Nature Materials,* **2016**, 15, 197-204.

[34] D. Voiry, M. Salehi, R. Silva, T. Fujita, M. Chen, T. Asefa, V. B. Shenoy, G. Eda, and M. Chhowalla, *Nano Lett.* **2013**, 13, 6222−6227.

.